

Synthesis and mechanical characterization of nanoparticle-infused polyurethane foams. Statistical analysis of foam morphology

D. V. Pikhurov¹, V. V. Zuev^{1,2}

¹ITMO University, Kronverkskiy pr., 49, 197101 St. Petersburg, Russia

²Institute of Macromolecular Compounds of the Russian Academy of Sciences,
Bolshoi pr., 31, 199004 St. Petersburg, Russia

nefaeron@gmail.com, zuev@hq.macro.ru

PACS 81.07.Lb

DOI 10.17586/2220-8054-2016-7-3-464-471

Nanocomposite polyurethane (PU) foams filled with different loadings (0.1 – 0.7 wt.%) of nanosized silica (average grain size of ~ 7 and 12 nm) and organonano clay were prepared by the prepolymer method, and their mechanical properties were investigated. A statistical analysis of the size distribution for foam cells was successfully applied in order to characterize their morphology. The developed approach was shown to provide a detailed analysis of the morphology development in PU foams, including the primary cell formation and their subsequent break-up and coalescence. The degree of phase separation in nanocomposite polyurethane foams, which is dependent on the nanofiller, was calculated from the IR spectra. The presence of silica nanoparticles and organoclays gives rise to significant differences in the mechanical (stress-strain) properties of the nanocomposite polyurethane foams relative to the pure polymer.

Keywords: polyurethane nanocomposite foams; nanosized silica; organoclay; microphase separation, statistical analysis.

Received: 25 February 2016

Revised: 4 April 2016

1. Introduction

Applications of polyurethane (PU) foams reach into various areas such as: lightweight materials, filtration and separation, biomaterials, electrochemical or catalyst support, heat and sound isolation [1]. These applications require a precise control of the PU foam's morphology to serve different purposes. A thorough description of the morphologies requires data such as cell size, their distribution, cell shape anisotropy, thickness of cell walls, size and shape of struts. One major aim of material science in this field is to improve or create new desirable properties for PU foams. A potential way to solve this problem is the creation of nanocomposites. The benefit of using of nanofillers is that their small amount is sufficient to induce tremendous improvements in desirable properties [2]. The morphology of PU foams synthesized by a phase separation process depends on many parameters, including the composition, type and amount of nanofillers. A quantitative understanding of the evolution of nanocomposite PU foam morphology may permit one to predict and control their properties.

Mathematical description with experimental validation and prediction of PU foam morphology is still scarce in the literature. Kim and Youn [3] and Bikard et al. [4] modelled the formation of PU foams and their characteristics. The mechanism for PU foam formation is complex because it includes phase separation into domains and the formation of gas phase from reacting polymer-monomer mixture. For these reasons, the developed models are phenomenological and allow only qualitative description of the process. The formation of PU foam cells assumes the random growth of cell on randomly-formed nucleates. This process can be described with the aid of kinetic model of reversible aggregation developed by Kilian et al. [5]. The model explains why aggregates of different size are generated across chemical/physical processes in a liquid system. The universality of the model has been shown by its application to statistical ensembles of carbon-black particles [5], spherulites in isotactic poly(methylmethacrylate) [5, 6], microdomains of polyamic acids during their transformation to polyimides [7], defects of metallographic samples under tensile loading [6], bacteria and yeast in the course of their growth [5], and the ordered phase droplets in liquid crystalline systems [8, 9], and in many other systems. A similar approach, we estimate, could successfully be applied to the formation of PU foams reinforced with nanofillers.

In the experimental part of this work, we use a mixture of forpolymer and polyol to create PU foams. We use nanoclay and nanosized silica as nanofillers. The prepared PU foams were investigated by image analysis and mechanical testing.

2. Experimental

2.1. Materials

The isocyanate used in this study was a polymeric aromatic isocyanate based on 4,4'-diisocyanate diphenylmethane (MDI) Wannate PM-200 from Yantai Wanhua (PR China) (molecular weight $M_n = 340$, 30.2 – 32 % NCO, viscosity at 25 °C 150 – 250 cps, specific gravity = 1.25 g/cc). As a rigid chain extender, methylenebis-(2-chloroaniline) (cuamine M) from Ihara Chemical Ind. (Japan) with $MM = 267$ was used. VORANOL 4711 polyether polyol from Dow Chemical (glycerine propoxylated ethoxylated polyol with $M_n = 4711$, OH number 32 – 37, viscosity at 25 °C 790 – 830 cps, specific gravity 1.021 g/cc) was used as the main polyol. As other polyols, VORANOL RA-640 polyether polyol from Dow Chemical (propoxylated ethylenediamine polyol with $M_n = 350$, OH number 640, viscosity at 25 °C 21000 cps, specific gravity 1.00 g/cc) and PDA-800 from Kazan SK (Russia) (polyester of adipic acid and polyethylene glycol with $M_n = 800$, OH number 400, viscosity at 25 °C 11000 cps, specific gravity 1.17 g/cc) were used. DMDEE (2,2'-dimorpholinodiethylether) from Hunstman was used as the catalyst. As nanoclays, montmorillonite (MMT) clay modified by cation exchange with long-chain (C16 – C18) quaternary ammonium Monamet 1P3 (has a particle size of less than 75 μm , interplate distance 37.5 Å, part of MMT is 80 %, specific gravity 0.45 g/cc) and Monamet 101 (has a particle size of less than 45 μm , interplate distance 41.6 Å, part of MMT is 80 %, specific gravity 0.40 g/cc) [10] from Metaclay (Russia) were used.

Aerosil*200 (has a mean particle size of 12 nm) and Aerosil*300 (has a mean particle size of 7 nm) from Evonik were utilized as the nanosized silica.

2.2. Synthesis of PU foams samples

MDI and polyol were dehydrated under vacuum overnight at room temperature and 60 °C respectively. All samples were prepared using the prepolymer technique [1]. A mixture of 63.9 wt.% of PM 200, 35.1 wt.% of VORANOL 4711 and 1 wt.% of oleic acid was used as the isocyanate prepolymer. A mixture of 58 wt.% of PDA-800, 38 wt.% of Cuamine A and 4 wt.% of VORANOL RA-640 was used as the polyol. The calculated amount of nanofiller was added to polyol and then magnetically stirred for at least 24 h.

The samples in this study were made by box foaming under a fume hood using an 18 × 18 × 12 cm steel box. A mixer with high rotation speed was used. The components in the formulation (13 g of isocyanate prepolymer and 13 g of polyol with nanoadditives) were mixed first for 3 s at 2400 rpm. Then, 0.5 g of 10 wt.% water solution of catalyst was added and immediately mixed for another 5 s at 2400 rpm. The blow off time occurs after the foam reaches maximum height. Once foaming is complete, the foam is further heated at 60 °C for 20 min, and then allowed to cure overnight under the fume hood. Foam sample walls (2.5 cm) are discarded, and the remaining samples are characterized.

2.3. Optical microscopy

A 2.0 cm × 2 cm × 2 mm piece was cut from the bulk with a razor blade. Diamond knife was used for microtomy. An optical microscope Micromed Met 400 (Micromed Met, Russia) with magnification up to 400 was used to analyze the surfaces of PU foams.

2.4. Fourier-transform infrared spectroscopy (FT-IR)

Attenuated total reflectance-infrared spectra were acquired using the Vertex Bruker Fourier-transform infrared spectrometer. A spectral resolution of 2 cm^{-1} was maintained, and 32 scans were co-added for acceptable signal-to-noise ratio. Diamond micro-ATR crystal accessory was used. Foam samples were placed between the crystal and a metal tip, and sufficient load was applied to ensure good contact of sample with the ATR crystal.

2.5. Mechanical testing

Mechanical testing was conducted using a TA.XTplus Texture Analyser.

2.6. Thermodynamic model using for statistical analysis

The model of reversible aggregation [5–7] was inspired by application of irreversible thermodynamics. It gives a generalized characterization of microstructure in different liquids. According to the model, a stationary microstructure is developed by linking the energy-equivalent units in metastable clusters called the aggregates. The aggregates are perpetually composed and decomposed under thermal fluctuations; this is a condition of their reversibility.

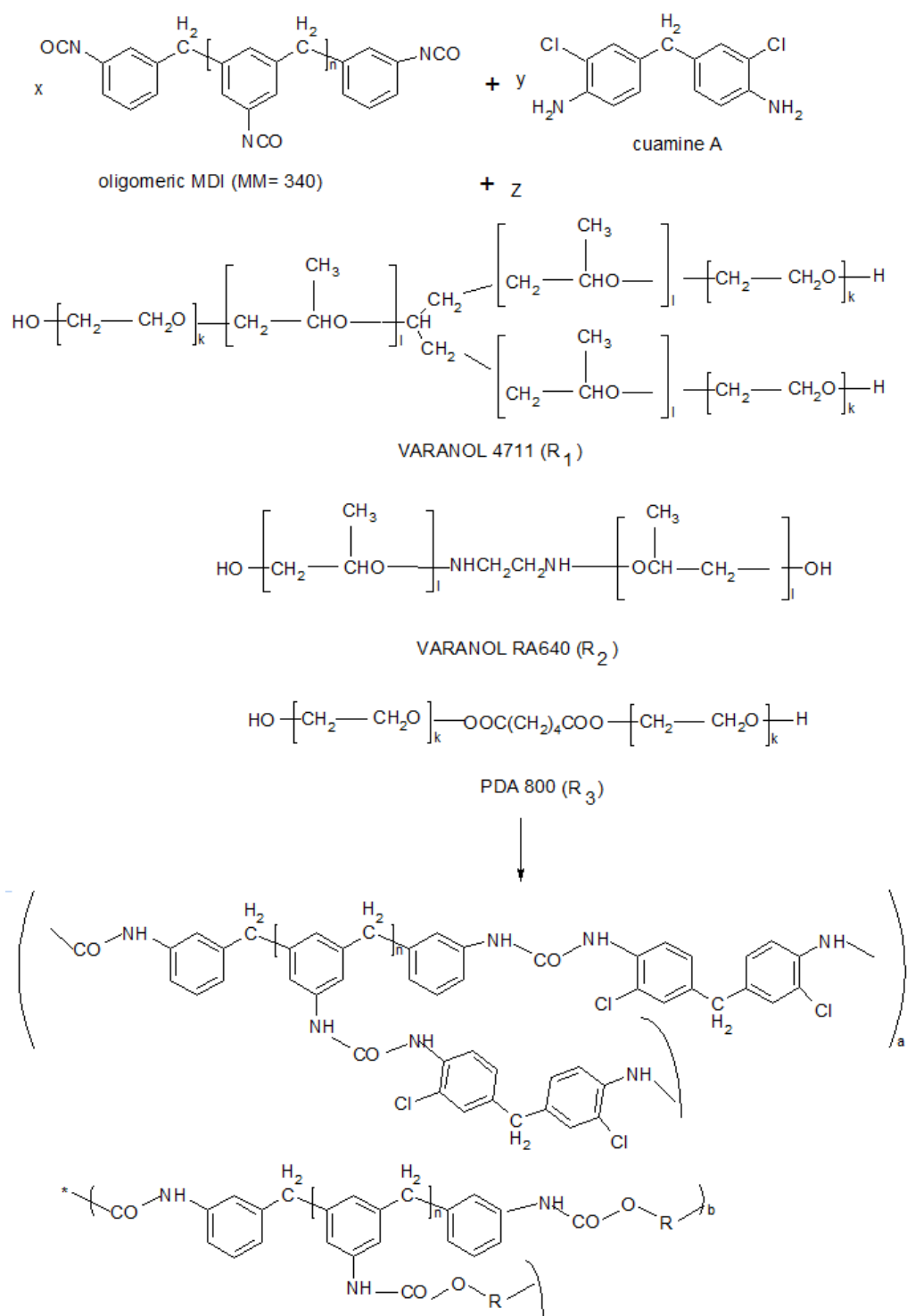


FIG. 1. Synthesis of PU foams samples

According to the model, the stationary statistical distribution $h(s)$ of the projected diameter s of the microstructural entities reads as follows [5–7]:

$$h(s) = as^2 \exp\left(-\frac{s\Delta u_0}{kT}\right), \quad (1)$$

where a is the normalizing factor, Δu_0 is the energy of aggregation, k is the Boltzmann constant, T is the absolute temperature, and k is the energy of thermal fluctuation. In some cases, the aggregates were shown to form not a single but rather multiple statistical ensembles [11]. This may be caused by either consolidation of primary clusters into superstructure (i.e. coalescence) or by the presence of different components in a multi-component system. Following this way, Eq. (1) should be written as [11]:

$$h(s) = \sum_{i=1}^N a_i s_i^2 \exp\left(-\frac{s_i \Delta u_{0i}}{kT}\right), \quad (2)$$

where N accounts for the total number of statistical ensembles of the entities. Eq. (2) allows the determination of the mean entity area $\langle s_i \rangle$ related to the i -th statistical ensemble as a normalized mathematical expectation:

$$\langle s_i \rangle = \frac{\int_{s_{0i}}^{\infty} s_i^3 \exp\left(-\frac{s_i \Delta u_{0i}}{kT}\right) ds_i}{\int_{s_{0i}}^{\infty} s_i^2 \exp\left(-\frac{s_i \Delta u_{0i}}{kT}\right) ds_i} = \frac{3kT}{\Delta u_{0i}}. \quad (3)$$

3. Results and discussion

PU foams were analyzed by optical microscopy in order to determine their morphology relative to the used nanofillers (Fig. 2). The cells basically appear spherical and closed. The purpose of optical microscopy analysis in the present paper is to determine the size of cells and their size distribution which will undoubtedly affect the performance of the resulting PU foams. The optical images obtained were subsequently segmented and subjected to digital analysis using the ImageTool 3.0 software elaborated at the Health Science Center (the University of Texas, San Antonio, USA) to elucidate the statistical size distributions of the dispersed phase droplets. To analyze the resulting histograms, we used the model of reversible aggregation. The area of each cell was then converted into the cell diameter for a circle with the area equivalent to the cell area. Let us note that we analyze a spatially 2D section of a foam sample and the equivalent cell diameters do not represent the real spatially 3D cell size.

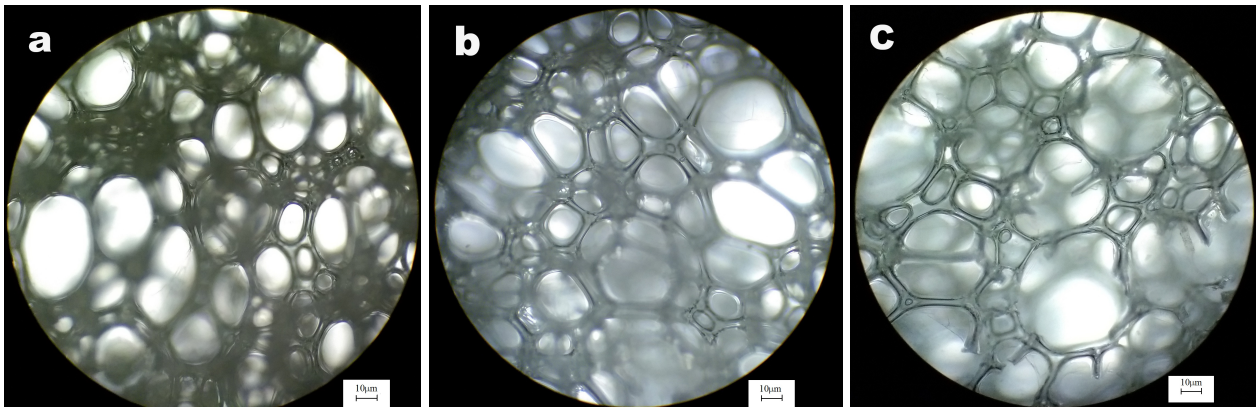


FIG. 2. Optical images of pristine PU foam (a); nanocomposite PU foam loaded with 0.08 wt.% of nanoclay Monamet 101 (b); nanocomposite PU foam loaded with 0.08 wt.% of nanosilica Aerosil*200 (c)

Two opposite processes determine the mean cell size during the PU foam formation process: break-up and coalescence. In order to investigate the evolution of cell size distribution during PU foam synthesis in the presence of different additives, statistical analysis of their diameters was undertaken. Our analysis is based on the model of reversible aggregation proposed by Kilian et al. [6] which has been successfully applied to describe the stationary phase distributions of microstructural entities in various systems. Fig. 3 shows the histograms obtained from the statistical analysis of the optical images of PU foams formed at different nanoparticle loadings (Fig. 2).

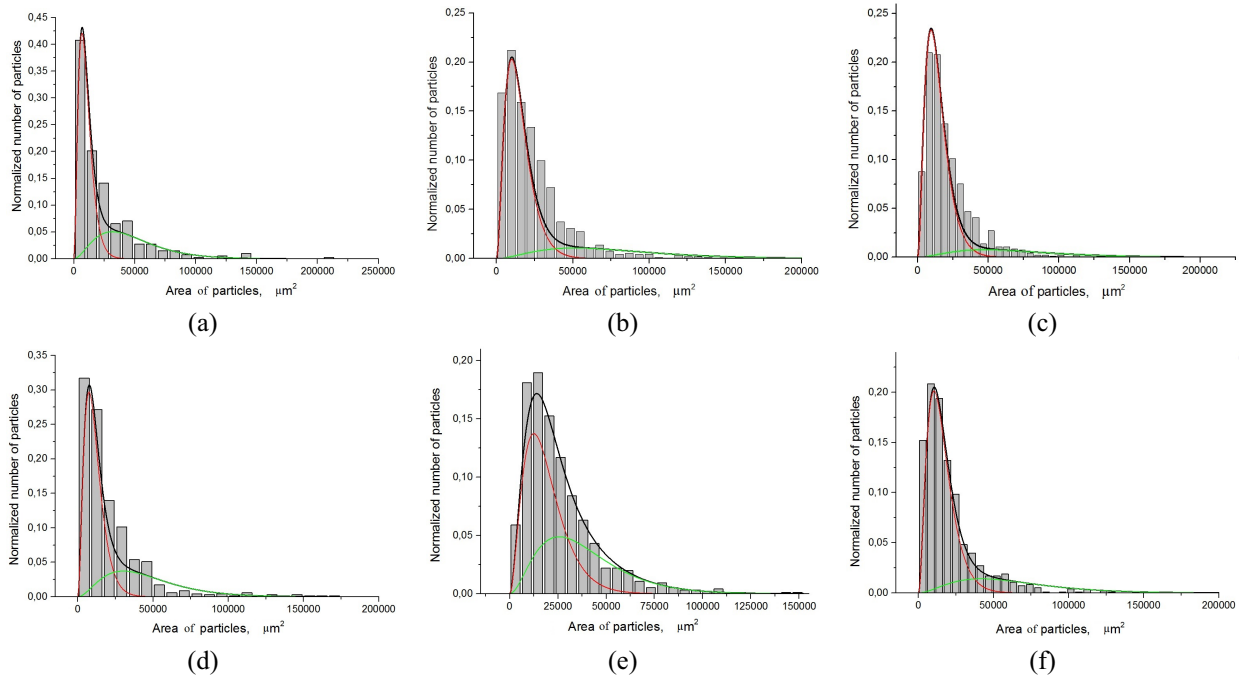


FIG. 3. Statistical distribution of cell area for pristine PU foam (a); nanocomposite PU foam loaded with 0.32 wt.% of nanoclay Monamet 101 (b); nanocomposite PU foam loaded with 0.32 wt.% of nanoclay Monamet 1P3 (c); nanocomposite PU foam loaded with 0.08 wt.% of Aerosil*200 (d); nanocomposite PU foam loaded with 0.63 wt.% of Aerosil*200 (e); nanocomposite PU foam loaded with 0.32 wt.% of Aerosil*300 (f)

Our attempt to describe the statistical ensembles with a unimodal version of the model of reversible aggregation (Eq. (1)) failed. Yet, we succeeded when we applied a bimodal version of the model (Eq. (2), $N = 2$). In Fig. 3, the dashed lines represent the individual distributions, whereas the solid lines represent the sum over two ensembles according to Eq. (2). A successful analytical description indicates that the PU foam cells form two superimposed, thermodynamically optimized, statistical ensembles of primary and coalescence cells all across the phase separation in the filled PU foams studied. We suggest the cells involved in the first statistical ensemble (i.e. small cells) were formed during the primary growth of PU foam synthesis, whereas the cells involved in the second statistical ensemble (big cells) resulted from coalescence.

The mean droplet diameter of each statistical ensemble as a function of the PU foam's compositions is given in Table 1.

As can be seen from Fig. 3, in the pristine PU foam, cells formed two superimposed, thermodynamically optimized, statistical ensembles of primary and coalesced cells. The mean cell size of each statistical ensemble can be assumed as a basic value when the influence of additives on PU foam morphology is analyzed. The first statistical ensemble contains not only primary cells but also droplets after break-up processes. As Fig. 2 and Table 1 show, the insertion of organoclay in the PU does not induce any modification of the cell morphology but led to a significant increase of the mean cell size in both statistical ensembles. For primary cells this, effect can be enhanced by residual water on the organoclay surface, which induces a supplementary CO_2 release. To the contrary, localization of nanoclay plates at the cell walls stimulates coalescence. The most common modeling of the mechanical behavior of cellular materials by the Gibson and Ashby approach [13] predicts that an increase of the cell dimensions should lead to a decrease of the foam's modulus. This view is supported by our measurements (Table 1). However, the mechanical response of these cellular materials also depends on the intrinsic properties of the polymer constituting the cell walls [1]. Morphology is the dominating factor determining the mechanical and many other properties of bulk PUs. PU is a multi-block copolymer that consists of alternating hard and soft segments. A hard segment (HS) consists of diisocyanate and chain extender, and a soft segment (SS) made from polyether or polyester polyol. The HS and SS are thermodynamically incompatible at low temperatures, resulting in the microphase separated structure of PU [14, 15]. The grade of the microphase separation can be determined from IR spectra using the part of free and hydrogen bonded carbonyl groups in urethane and urea bonds [16]. The FTIR spectra of the pristine and nanofilled PU foams and are shown in Fig. 4.

TABLE 1. Effect of loading on the properties of the nanocomposite PU foams

Loading, wt. %	Young's modulus (E), GPa	Tensile strength σ , MPa	Mean cell diameter, μm ; 1 ensemble	Mean cell diameter, μm ; 2 ensemble	Fraction of 1 ensemble	Fraction of hydrogen bonded urethane bond	Fraction of hydrogen bonded urea bond
pristine	4.59±0.02	0.51±0.01	113	246	1.75	0.93	0.37
Monamet 101							
0.08	4.05±0.02	0.50±0.01	145	330	3.2	0.74	0.25
0.16	3.93±0.02	0.48±0.01	141	330	2.7	0.64	0.27
0.32	3.98±0.02	0.49±0.01	138	313	3.7	0.79	0.19
0.63	3.63±0.02	0.41±0.01	150	276	2.5	0.98	0.24
Monamet 1P3							
0.08	4.35±0.02	0.55±0.01	145	301	4.2	0.82	0.43
0.16	4.13±0.02	0.52±0.01	159	301	4.6	0.77	0.55
0.32	3.98±0.02	0.50±0.01	134	301	6.1	0.71	0.56
0.63	3.65±0.02	0.46±0.01	126	340	1.6	0.83	0.41
Aerosil* 200							
0.08	3.96±0.02	0.52±0.01	154	221	1.4	0.78	0.52
0.16	4.67±0.02	0.62±0.01	141	221	1.7	0.81	0.52
0.32	4.60±0.02	0.61±0.01	131	215	1.6	0.75	0.48
0.63	4.12±0.02	0.54±0.01	119	240	1.9	0.76	0.50
Aerosil* 300							
0.08	4.67±0.02	0.62±0.01	126	242	3.2	0.85	0.51
0.32	3.68±0.02	0.49±0.01	140	252	3.5	0.86	0.50
0.63	4.15±0.02	0.55±0.01	134	242	2.5	0.77	0.41

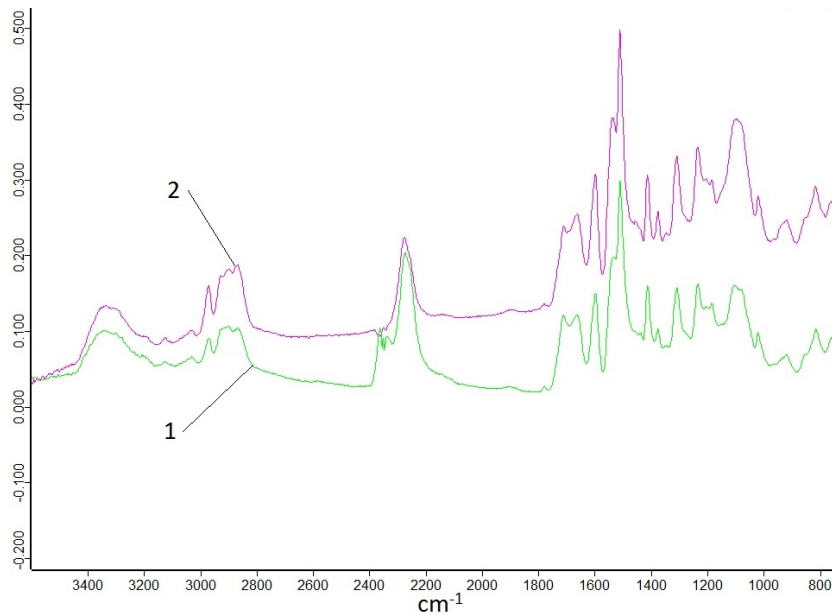


FIG. 4. IR spectra of pristine PU foams (1) and nanocomposite PU foam loaded with 0.32 wt.% of nanoclay Monamet 101 (2)

They are very similar, except in some regions that will be specified below. The positions of the bands characteristic of the functional groups remain the same in all the samples. We are able to derive the peaks of (-N=C=O), (-O-H) and (H-N=C=O). It should be noted that -NCO vibration (2270 – 2280 cm⁻¹), -NH vibration (3360 – 3380 cm⁻¹) and -OH vibration (3530 – 3550 cm⁻¹) are the most important peaks. Other important peaks

are urethane -C=O vibration ($1740 - 1700 \text{ cm}^{-1}$) and urea -C=O vibration ($1680 - 1640 \text{ cm}^{-1}$). However, there are significant differences concerning the band intensities in the C=O ($1750 - 1600 \text{ cm}^{-1}$) region (Fig. 5).

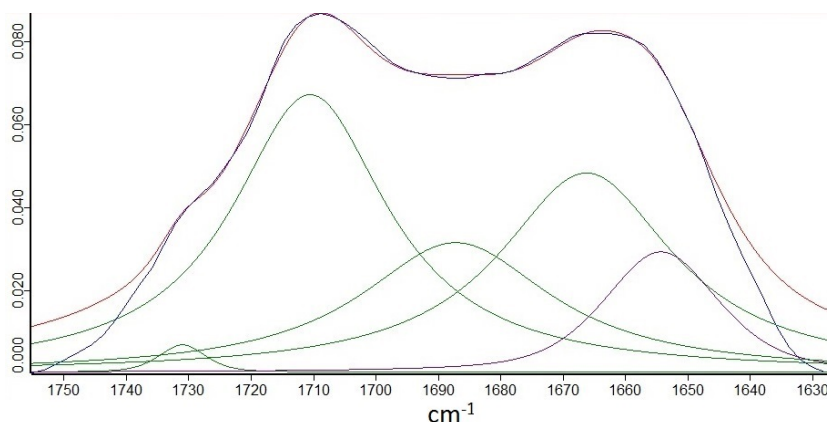


FIG. 5. Deconvolution of bands in IR spectrum of nanocomposite PU foam loaded with 0.32 wt.% of nanoclay Monamet 101 in the region of C=O groups stretching

The former region is characteristic of hard segments. The urethane and urea groups take part in the formation of hydrogen bonds. In a pure PU foams, two types of hydrogen bonds can be formed between NH groups and proton accepting oxygen in (i) urethane C=O groups, and (ii) urea C=O groups. The type and the strength of the hydrogen bonds are usually recognized by the magnitude of the wave number shifts. Traditionally, the $\text{N-H}\cdots\text{O=C}$ hydrogen bond between two urea groups has been considered the strongest, with hydrogen bond between two urethane groups being the second strongest. However, recent studies have shown that $\text{N-H}\cdots\text{O}$ (ether) bond is slightly stronger than $\text{N-H}\cdots\text{O=C}$ urethane bond [16]. Conversely, it is known that the primary hydrogen bond acceptor depends on the length the soft segments and the concentration of the hard segments in a chain [17]. FTIR spectra in the carbonyl stretching region are presented in Fig. 5. All the spectra were resolved into five spectral components, the one at 1711 cm^{-1} was assigned to the hydrogen bonding between hard segments and urethane carbonyl groups. The other band at 1734 cm^{-1} corresponds to the stretching vibration of free carbonyl group of urethane bond of hard segments. Similarly, the band at 1644 cm^{-1} was assigned to the hydrogen bonding between hard segments and urea carbonyl groups. The band at 1664 cm^{-1} corresponds to the stretching vibration of free carbonyl group of urea bond of hard segments. The fifth band at 1644 cm^{-1} can be assigned to the allophanate formed as a by-product during the synthesis of PU foams [18].

The microphase separation can be characterized by the degree of phase separation (DPS) that is generally evaluated by the following relation:

$$DPS = \frac{A_b}{A_f + A_b}, \quad (4)$$

where A_b and A_f are the integrated absorbances (ε_b and ε_f are extinction coefficients which are assumed equal, although the actual value of $\varepsilon_b/\varepsilon_f$ is probably between 1.0 and 1.2 [16]) of hydrogen bonded and free molecular group, respectively. In other words, the limiting values of DPS, i.e. 0 and 1, refer to the single phase systems. The C=O bands were deconvoluted using Gaussian shape and the obtained values of DPS for PU foam, as well as for their nanocomposites are given in Table 1. The fraction of hydrogen bonded carbonyls equal to DPS is a measure of phase separation, i.e. it relays information on the occurrence and the size of the hard domains. It is known that in pure PU hydrogen bonded components are expected only in hard domains, while the free ones can exist only dispersed in soft domains or in the interphase. Our data for the pristine PU foam supports this model. The DPS for urethane bonds is 0.93 which suggests that their location is in the hard domains. The DPS for urea bonds is 0.37, suggesting that their location is primarily in the interphase. The difference of DPS values for urethane and urea bonds can be explained by the fact that reactivity of cuamine A leads to location of urea groups on the ends of hard segments. The introduction of organoclay in PU foams leads to a decrease in DPS values. The organoclay, which can form hydrogen bonds with urethane and urea bonds, destroys the hard domains and softens the PU cell walls. This, along with increasing the cell diameter in both statistical ensembles, also explains the decrease in the mechanical properties of PU nanocomposite foams filled with organoclay.

A similar situation was observed for PU nanocomposite foams filled with nanosized silica (Table 1). The silica have hydrophilic surface and can forms hydrogen bonds with urethane and urea bonds. As a result, the DPS

for urethane bonds for PU nanocomposite foams filled with nanosized silica are lower than for pristine PU foam. However, the DPS for urea bonds is rather more that can be associated solely with formation of hydrogen bonds with silica.

The PU nanocomposite foam cells filled with nanosized silica also form two statistical ensembles of primary and coalescence cells (Fig. 3). However, the mean cell diameter for second statistical ensemble is practically identical for nanocomposites filled with Aerosil*300 and lower for nanocomposites filled with Aerosil*200 than for pristine PU foam (Table 1). As result, these nanocomposites have mechanical properties similar to pristine PU foam. Thereby, the hydrophilic nanosized filler such silica and organoclay can change supramolecular structure of PU and supervise the cell formation during PU foam synthesis, therefore, allowing one to predetermine the foams' mechanical properties.

4. Conclusions

A statistical analysis of the cell sizes was successfully applied to characterize the morphology of pristine PU foams and nanocomposite PU foams filled with nanosized silica or organoclay. The cells were shown to form two superimposed, thermodynamically optimized, statistical ensembles of primary and coalesced cells all across the phase separation in the foam manufacturing processes studied. The mean cell size of each ensemble was assumed as the basis for analysis of the influence of additives on nanocomposite PU foam morphology. The addition of organoclay led to a significant increase in the mean cell size both statistical ensembles. Hence, the introduction of organoclay decreases the break-up of primary cells and stimulate their coalescence. The addition of nanosized silica, contrary to nanoclay, did not stimulate coalescence but the mean cell size in both statistical ensembles was reduced. The development of phase morphology influences the mechanical properties of PU foams strongly.

The comprehensive IR study showed that in the case when the particles of the nanofiller can form hydrogen bonds with polymer segments, it is necessary to analyze changes due to the hydrogen bonding in foam phase structure. The loading hydrophilic nanofiller in PU foams lead to a decrease in the microphase separation that leads to decreased mechanical strength.

References

- [1] Yang C., Fischer L., Maranda S., Worlitschek J. Rigid polyurethane foams incorporated with phase change materials: A state-of-the-art review and future research pathways. *Energy and Buildings*, 2015, **97**, P. 25–38.
- [2] Mahfuz H., Rangari V.K., Islam M.S., Jeelani S. Fabrication, synthesis and mechanical characterization of nanoparticles infused polyurethane foams. *Composites: Part A*, 2004, **35**, P. 453–460.
- [3] Kim C., Youn J.R. Environmentally friendly processing of polyurethane foam for thermal insulation. *Polym. Plast. Technol. Eng.*, 2000, **39**, P. 163–185.
- [4] Bikard J., Bruchon J., Coupez T., Vergnes B. Numerical prediction of the foam structure of Polymeric materials by direct 3D simulation of their expansion by chemical reaction based on a multidomain method. *J. Mater. Sci.*, 2005, **40**, P. 5875–5881.
- [5] Kilian H.G., Metzler R., Zink B. Aggregate model of liquids. *J. Chem. Phys.*, 1997, **107**, P. 8697–8705.
- [6] Kilian H.G., Köpf M., Vettegren V.I. Model of reversible aggregation: universal features of fluctuating ensembles. *Progr. Colloid Polym. Sci.*, 2001, **117**, P. 172–181.
- [7] Kilian H.G., Bronnikov S., Sukhanova T. Transformation of the micro-domain structure of polyimide films during thermally induced chemical conversion: characterization via thermodynamics of irreversible processes. *J. Phys. Chem. B*, 2003, **107**, P. 13575–13582.
- [8] Zuev V.V., Bronnikov S. Stationary statistical size distribution of nematic droplets in the course of the isotropic liquid-nematic phase transition. *Liq. Cryst.*, 2008, **35**, P. 1293–1298.
- [9] Bronnikov S., Kostromin S., Zuev V.V. Kinetics of the isotropic-nematic phase transition in the melted multi-component liquid crystal mixtures upon cooling. *Phase Trans.*, 2010, **83**, P. 302–308.
- [10] Bachov F.I., Cherkina U.Yu., Shtepa S.V. The method of preparation of gem-organomodified montmorillonite with high thermal stability. Patent 2519174 (2013), Russia.
- [11] Zuev V.V., Steinhoff B., et al. Flow-induced size distribution and anisotropy of the minor phase droplets in a polypropylene/poly (ethylene-octene) copolymer blend: Interplay between break-up and coalescence. *Polymer*, 2012, **53**, P. 755–760.
- [12] Gibson L.J., Ashby M.F. *Cellular solids: Structure & properties*. Pergamon Press, Oxford, 1988, 357 p.
- [13] Chattopadhyay D.K., Raju K.V.S.N. Structural engineering of polyurethane coatings for high performance applications. *Prog. Polym. Sci.*, 2007, **32**, P. 352–418.
- [14] Bandekar J., Klima S. FT-IR spectroscopic studies of polyurethanes Part II. Ab initio quantum chemical studies of the relative strengths of “carbonyl” and ether hydrogen-bonds in polyurethanes. *Spectrochim. Acta A*, 1992, **48**, P. 1363–1370.
- [15] Mokeev M.V., Zuev V.V. Rigid phase domain sizes determination for poly(urethane-urea)s by solid-state NMR spectroscopy. Correlation with mechanical properties. *Eur. Polym. J.*, 2015, **71**, P. 372–379.
- [16] Sun H. Ab initio characterizations of molecular structures, conformation energies, and hydrogen-bonding properties for polyurethane hard segments. *Macromolecules*, 1993, **26**, P. 5924–6.
- [17] Seymour R.W., Estes G.M., Cooper S.L. Infrared studies of segmented polyurethane elastomers. I. Hydrogen bonding. *Macromolecules*, 1970, **3**, P. 579–83.
- [18] Yilgor E., Yilgor I., Yurtsever E. Hydrogen bonding and polyurethane morphology. I. Quantum mechanical calculations of hydrogen bond energies and vibrational spectroscopy of model compounds. *Polymer*, 2002, **43**, P. 6551–9.